Journal of Quantitative Spectroscopy & Radiative Transfer 122 (2013) 3–12

Contents lists available at SciVerse ScienceDirect

Journal of Quantitative Spectroscopy & Radiative Transfer

journal homepage: www.elsevier.com/locate/jqsrt

Macrophysical and optical properties of mid-latitude cirrus clouds over a semi-arid area observed by micro-pulse lidar

Jin Wang, Lei Zhang*, Jianping Huang, Xianjie Cao, Ruijin Liu, Bi Zhou, Hongbin Wang, Zhongwei Huang, Jianrong Bi, Tian Zhou, Beidou Zhang, Tengjiao Wang

Key Laboratory for Semi-Arid Climate Change of the Ministry of Education, College of Atmospheric Sciences, Lanzhou University, Tianshui South Road 222, Lanzhou 730000, China

ARTICLE INFO

Article history:
Received 3 July 2012
Received in revised form
27 December 2012
Accepted 11 February 2013
Available online 18 February 2013

Keywords:
Mid-latitude cirrus
Micro-pulse lidar
Optical depth
Lidar ratio
Semi-arid area

ABSTRACT

Macrophysical and optical characteristics of cirrus clouds were investigated at the Semi-Arid Climate Observatory and Laboratory (SACOL; 35.95°N, 104.14°E) of Lanzhou University in northwest China during April to December 2007 using micro-pulse lidar data and profiling radiometer measurements. Analysis of the measurements allowed the determination of macrophysical properties such as cirrus cloud height, ambient temperature, and geometrical depth, and optical characteristics were determined in terms of optical depth, extinction coefficient, and lidar ratio. Cirrus clouds were generally observed at heights ranging from 5.8 to 12.7 km, with a mean of 9.0 ± 1.0 km. The mean cloud geometrical depth and optical depth were found to be 2.0 ± 0.6 km and 0.350 ± 0.311, respectively. Optical depth increased linearly with increasing geometrical depth. The results derived from lidar signals showed that cirrus over SACOL consisted of thin cirrus and opaque cirrus which occurred frequently in the height of 8–10 km. The lidar ratio varied from 5 to 70 sr, with a mean value of 26 ± 16 sr, after taking into account multiple scattering effects. The mean lidar ratio of thin cirrus was greater than that of opaque cirrus. The maximum lidar ratio appeared between 0.058 and 0.3 when plotted against optical depth. The lidar ratio increased exponentially as the optical depth increased. The maximum lidar ratio fell between 11 and 12 km when plotted against cloud mid-height. The lidar ratio first increased and then decreased with increasing mid-height.

1. Introduction

In the past two decades, many studies reveal that cirrus clouds play a crucial role in the radiation budget of the earth-atmosphere system [1–3]. The influence of cirrus clouds on the climate of the upper troposphere is important, not only because cirrus appear at high altitudes, but also because they consist of non-spherical ice crystals with complicated absorption and scattering properties. Cirrus clouds are widely dispersed in the upper troposphere and regularly cover about 20% of the total earth's surface [4].

Cirrus clouds play an important part in modulating regional and global climate via two complex processes. One is the albedo effect in which high-altitude cirrus clouds can scatter or absorb solar radiation, cooling the Earth's surface by reflecting solar insolation; the other is the greenhouse effect, which results in atmospheric warming due to the trapping of longwave radiation [5,6]. Liou [1] suggested that tropical cirrus acts as a greenhouse modulator, whereas the albedo effect is more effective in mid-latitude cirrus. Fu and Liou [7] reported

* Corresponding author.
E-mail address: zhanglei@lzu.edu.cn (L. Zhang).

0022-4073/$ - see front matter © 2013 Elsevier Ltd. All rights reserved.
http://dx.doi.org/10.1016/j.jqsrt.2013.02.006

that thin clouds may cause a positive radiative forcing at the top of the atmosphere, whereas thick cirrus clouds produce cooling. Additionally, cirrus clouds are crucial to the hydrological cycle of the atmosphere and to stratosphere–troposphere exchange (STE) processes for water vapor. The parameterization of cirrus in terms of their macrophysical and optical characteristics at different geographic locations is very important for climate models and particularly in the improvement of the general circulation model (GCM) due to their important roles in climate, radiation balance, and water vapor exchange.

However, significant uncertainties remain regarding the radiative and climatic effects of cirrus clouds [8] and subsequent predictions of the changing global climate. Consequently, studies on cirrus are currently being undertaken worldwide. In an attempt to assess the impact of clouds on the global climate, many experiments such as the First ISCCP (International Satellite Cloud Climatology Project) Regional Experiment (FIRE), Cirrus Intensive Observations (IFO) [9], the European experiments on cirrus (ICE/EUCREX) [10], and the Experimental Lidar Pilot Study (ECLIPS) [11] have been conducted using a variety of techniques to investigate and improve our knowledge of cirrus clouds and their radiative properties in different regions of the globe.

Today, there are several global and regional networks of atmospheric observatories that use lidar as their main monitoring instrument because of the high spatial and temporal resolution it provides. The lidar technique has become a quantitative tool for detecting and characterizing cirrus clouds from the ground (ground-based lidar). Extensive ground-based measurements have been undertaken to study the geometrical and optical properties of tropical high-altitude cirrus and their radiative properties by various research groups in the tropics [12–14]. Similarly, cirrus clouds have also been widely observed at mid-latitudes. A ground-based lidar and a passive radiometer have been used together to remotely sense the gross structure and optical properties of cirrus, both at mid-latitudes and in the tropics [15]. Using a UV Raman lidar at Geesthacht (53.5°N, 10.5°E) in northern Germany, Reichardt [16] reported that cirrus mid-cloud height and temperature yielded distribution maxima between 9 and 10 km and between −50 and −60 °C, respectively. Sassen and Cambell [17] determined the cirrus cloud base/top properties to be 8.79/11.2 km and −34.4/−53.9 °C from 10-yr extensive high-cloud datasets collected from the University of Utah campus (40.8°N, 111.8°E). Xue et al. [18] showed that the peak appearance of high-altitude cirrus over Hefei, Anhui (31.90°N, 117.16°E), observed by L300 Mie lidar ranges from 8 to 11 km. Giannakaki et al. [19] found that cirrus clouds are generally observed over Thessaloniki, Greece (40.6°N, 22.9°E) at heights ranging from 8.6 to 13 km, with mid-cloud temperatures in a range from −65 to −38 °C.

It should be noted that cirrus climatology observed by a ground-based lidar over one particular location cannot be considered globally representative. Although the macrophysical and optical properties of cirrus clouds over north China were described by the lidar observations from the Earth-orbiting Cloud-Aerosol Lidar with Orthogonal Polarization (CALIOP) instrument on board the Cloud-Aerosol Lidar and Infrared Pathfinder Satellite Observations (CALIPSO) satellite [20], the ground-based lidar observations could provide more continuously intensive measurements, comparing with the satellite observations of cirrus, so that more accurate properties could be retrieved [21,22].

The semi-arid area of northwest China is still lacking in lidar observations of cirrus clouds. Therefore, to understand the morphology and effects of cirrus clouds in this region, this study was designed to determine the statistical characteristics of cirrus clouds during the period from April to December 2007 by using ground-based micropulse lidar (MPL-4B) measurements at the Semi-Arid Climate Observatory and Laboratory (SACOL, 35.95°N, 104.14°E) of Lanzhou University in northwest China. The macrophysical and optical characteristics of cirrus clouds over SACOL are discussed here in detail and are also compared with other studies made over different geographic locations.

2. Instrumentation

The Semi-Arid Climate Observatory and Laboratory (SACOL) is a permanent cloud-research station located on the western edge of Lanzhou University (35.95°N, 104.14°E) at the top of Tsuiying mountain (about 1965.8 m above sea level). It was established in 2005. This site is approximately 48 km from the city of Lanzhou, which is situated on the southern bank of the Yellow River in the Gansu province in Northwest China [23]. The elastic-scattering MPL-4B system used for performing continuous measurements of suspended aerosol particles and cirrus clouds in this study was installed at SACOL in 2007. Its significant eye-safety feature compared with standard lidar systems is achieved by using low pulse energies and high pulse repetition rates. The lidar is equipped with an Nd: YLF laser pointed vertically, emitting a micro-pulse of 8 μJ output energy at a wavelength of 527 nm and a 2500 Hz repetition rate. The optical receiver is a Cassegrain telescope of 178 mm diameter with a field of view of 0.1 mrad. The vertical resolution of the elastic raw signal at 527 nm is equal to 75 m.

We defined the "effective height" as the height where the number of bins with negative signal intensity is larger than 5 in a 10-point bin. In order to obtain the accurate properties of cirrus, the signal is considered to be too noisy for further analysis when the effective height of the lidar signal falls below 15 km. Moreover, one cloud profile was generated by a one-minute lidar measurement time; hence, a measurement period of a few hours often resulted in hundreds of profiles. Because of the variable nature of cirrus clouds, ten profiles were averaged to produce one lidar ratio for a cirrus cloud. There were 1042 data points in total produced from April to November 2007.

3. Data analysis

Hu et al. [24] have found that the fraction of supercooled water is higher at higher latitudes than at lower latitudes for the same mid-layer cloud temperature. The

presence of supercooled water clouds is very low between 40°S and 40°N, except over China. Due to the sulfate particles in polluted air may coagulate with ice-forming nuclei and deactivate them, the ice-forming nuclei reduce. In addition, many more supercooled water clouds in China are observed during winter and spring seasons. Besides, Doutriaux-Boucher and Quaas [25] have performed a multitude of short model integrations and derived a best estimate for the lowest local temperature where liquid water can exist in a cloud ($T_{ice}=-32$ °C). Houze [26] suggests a range of T_{ice} between −35 °C and −40 °C.

Although Lanzhou is polluted heavily during winter and spring seasons, the period of the data used in my study is from April to November, mainly containing summer and fall seasons. According to the reasons given above, in our study, only clouds with mid-cloud temperature below −38 °C are considered in order to avoid a possible impact of water clouds to our measurements.

Giannakaki et al. [19] have studied the optical and geometrical characteristics of cirrus clouds with temperature below −38 °C over Thessaloniki, Greece (40.6°N, 22.9°E). Liu et al. [27] obtained an annually averaged ambient temperature profile over a semi-arid area and found that the base height of cirrus cloud should exceed 6 km. However, because of strong seasonal variations in ambient temperature at mid-latitudes, the profiles for every month were averaged to produce annual temperature profiles, and we considered the height where the ambient temperature is less than −38 °C to be the base height for the corresponding month. Table 1 summarizes the height where −38 °C was recorded from May to December 2007. The information regarding the vertical distribution of ambient temperature was obtained from a profiling radiometer (TP/WVP-3000). Table 1 show that a maximum height for −38 °C of 8.2 km above ground level (AGL) occurred in July. For seasonal reasons, the height in summer was distinctly higher than that in other seasons. The lowest height for −38 °C of 4.8 km occurred in winter.

To obtain reliable, quantitative measurements of the optical properties of cirrus clouds such as optical depth, the correct boundary of the cloud must be determined. For this reason, the "threshold" method developed by Platt et al. [11] was employed to obtain cirrus clouds boundaries in this study. The cloud-base height is defined as the point at which there is an increase in lidar signal level equal to twice the standard deviation of the fluctuations above the background level. The lidar signal is required to increase continuously, or not to decrease, for at least five height intervals. When the fluctuations in signal below the cloud base are close to zero, any measurable increase defines the actual cloud base. Cloud-top height can also be determined by calculating the standard deviation of noise above the cloud top and moving downwards [11]. The cirrus mid-cloud height is defined as

$$Z_{mid}=\frac{\int_{Z_b}^{Z_t} zR_e(z)dz}{\int_{z_b}^{Z_t} R_e(Z)dz} \tag{1}$$

where Z_t and Z_b represent the cloud-top and cloud-base height, respectively. $R_e(z)$ is the backscattering ratio, which is given by

$$R_e(z)=\frac{\beta(z)+\beta_{air}(z)}{\beta_{air}(z)} \tag{2}$$

where $\beta(z)$ and $\beta_{air}(z)$ are the backscatter coefficients of aerosols and molecules at slant range Z, respectively.

From Rayleigh scattering theory, the ratio for the molecular scatterers is the constant $S_{air}=\sigma_{air}/\beta_{air}=8\pi/3$. The corresponding parameters for clouds, i.e., the backscatter coefficient $\beta(z)$ and extinction coefficient $\sigma(z)$, are both unknown, but are related by the extinction-to-backscattering ratio, namely, lidar ratio S_c, as defined by Eq. (3).

$$S_c=\sigma/\beta \tag{3}$$

The optical depth τ and transmission T can be determined by the following equations:

$$\tau=\int_{Z_b}^{Z_t}\sigma(z)dz \tag{4}$$

$$T=\exp(-\tau) \tag{5}$$

Although lidar has the potential for making remote measurements of atmospheric extinction with excellent spatial and temporal resolution, an accurate inversion of the lidar equation imposes stringent requirements for understanding the lidar ratio in order to retrieve the backscatter coefficient. So for the present analysis, we applied the transmittance method [19,29] to derive optical properties of cirrus clouds. We should mention that the accuracy of transmittance method for dealing with cirrus clouds and multiple scattering contributions relies on signal-to-noise ratio (SNR) and cleanliness of background aerosol. The cloud transmission or optical depth was determined by comparing the signals at the cloud base and top. The error of the optical depth was therefore proportional to the signal-to-noise that can be represented by the following expression:

$$\delta\tau\approx\frac{1}{2}\left[\frac{\Delta P_{top}^2}{P_{top}^2}+\frac{\Delta P_{base}^2}{P_{base}^2}\right]=\left[\frac{1}{SNR_{top}^2}+\frac{1}{SNR_{base}^2}\right] \tag{6}$$

This method works better for cloud with optical depth greater than about 0.05 [29]. Large errors were generated for thin clouds. So the lidar observations were carried out during the night time only because the influence of solar light on observations in the daytime, the signal-to-noise ratio was relatively very poor.

Multiple scattering is important in cirrus clouds and varies with cloud optical depth and cloud extinction. For clouds with optical depth higher than 0.1, multiple scattering must be considered because it alters the cloud optical properties [28]. Wang et al. [28] reported that the existence of multiple scattering can result in an underestimation of the extinction coefficient by 200%; however, the backscattering coefficient is almost unaffected. The

Table 1
Height at −38 °C from May to December 2007.

Month	May	Jun.	Jul.	Aug.	Sept.	Oct.	Nov.	Dec.
−38 °C height AGL (km)	7.5	7.5	8.2	8.0	7.2	6.9	5.4	4.8

approach for the correction of the estimated values of cirrus optical depth and lidar ratio depends on the method applied. For the transmittance method we assume a range-independent parameter. Following previous studies [15,22,29], a factor η was introduced that describes the multiple-scattering effect, henceforth termed the multiple-scattering factor. According to Chen et al. [29], the multiple scattering factor is calculated by Eq. (7).

$$\eta = \frac{\tau}{\exp(\tau) - 1} \tag{7}$$

The smaller the value of η is, the more important the multiple-scattering effect becomes. However, this approach is very simplistic because the multiple-scattering factor is only dependent on optical depth.

4. Results and discussion

4.1. Macrophysical characteristics

During the period from April to November 2007, 1042 samples of cirrus clouds were selected to study the cirrus climatology over SACOL.

Fig. 1(A) presents the relative probability distribution of the measured cloud-base height. Cirrus cloud-base height ranged from 4 to 13 km (AGL). The cloud-base height was mostly between 5 and 10 km (97.8% of measurements). The cloud-base height yielded a distribution maximum between 7 and 8 km, with 37.4% of measurements being in this range. Fig. 1(A) also indicates that only 0.2% of our samples had a cloud-base height between 4 and 5 km, whereas 0.2% of samples were above 12 km, with the data presented as a normal distribution. Fig. 1(B) presents the probability density functions for the cloud-top height, showing that 92.7% of samples had a cloud-top height in the range of 8 to 12 km; 74% had a cloud-top height between 9 and 11 km. Fig. 1(C) presents the distribution of the cirrus mid-cloud height over SACOL. Cirrus clouds were generally observed in the mid-latitude region from 5.8 to 12.7 km, with a maximum between 8 and 10 km. Of the samples, 93.5% had a mid-cloud height between 7 and 11 km. A histogram of cloud geometrical thickness is presented in Fig. 1(D). The thickness of cirrus cloud was confined to a range of 0.8 – 4.0-km, with a mean value of 2.0 ± 0.6 km. In 77.3% of the samples, the thickness of cirrus clouds was between 1.0 and 2.5 km. The maximum geometrical depth fell between 3.5 and 4.0 km, and the minimum occurred in

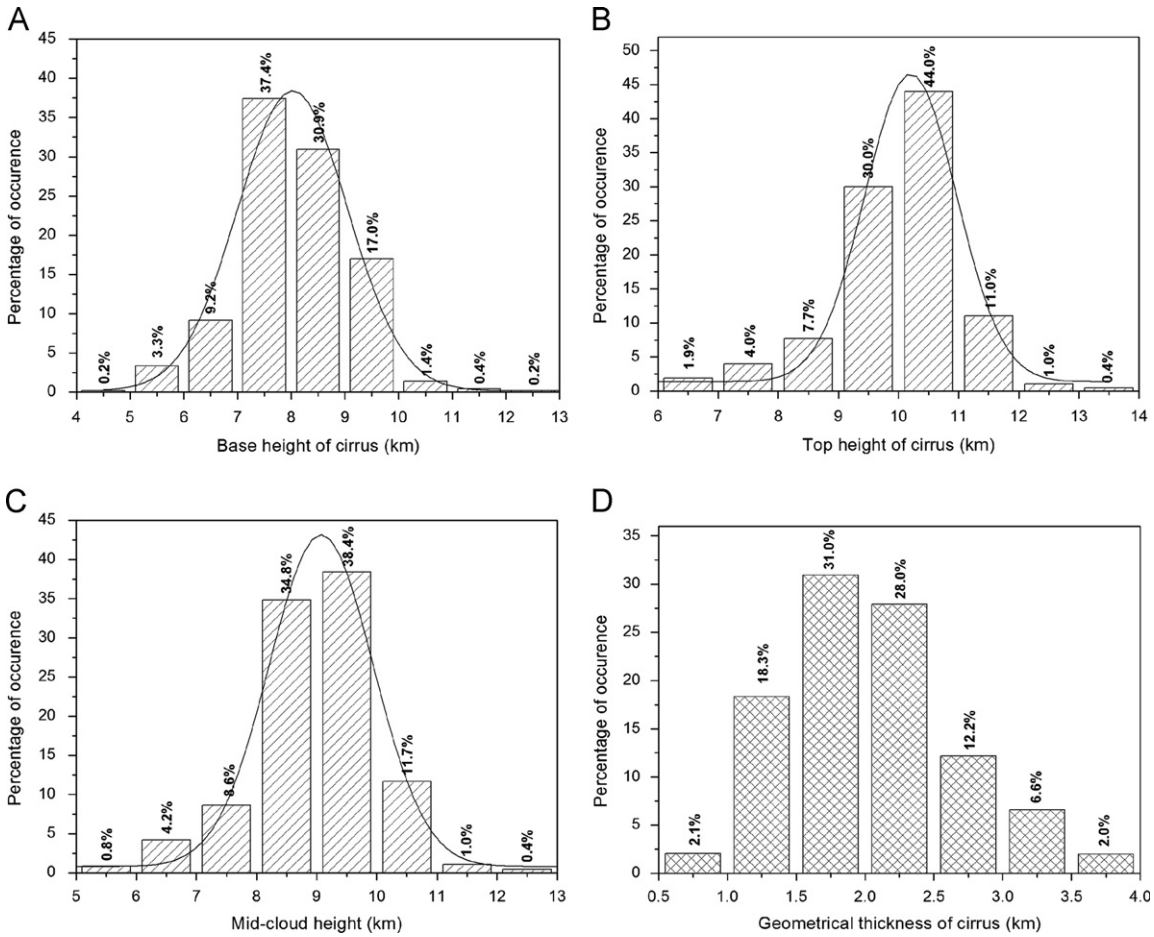

Fig. 1. Frequency occurrence at 1-km intervals of cirrus height for cloud-base height (A), cloud-top height (B), mid-cloud height (C), and the relative frequency distribution of cirrus geometrical thickness at 0.5-km intervals (D). % indicates the percentage of occurrence of cirrus.

Table 2
Mean values and standard deviation (parentheses) of cirrus macrophysical properties.

	Location	Cloud-top height (km)	Cloud-base height (km)	Geometrical depth (km)
Prestwick, Scotland [30]	55.5°N, 4.6°W	9.6	8.3 (8.5)	1.2
Haute Provence, France [31]	44°N, 6°E	10.7	9.3	1.4
Salt Lake City, USA [17]	40.8°N, 111.8°E	11.2	8.79	1.81
Thessaloniki, Greece [19]	40.6°N, 22.9°E	13	8.6	2.7 (0.9)
Lanzhou, China	35.95°N, 104.14°E	10.0 (1.1)	8.0 (1.0)	2.0 (0.6)
Chung-Li, Taiwan [32]	24.58°N, 121.10°E	14.43 (1.9)	12.34 (2.2)	2.08 (1.2)
Hulule, Maldives [33]	4.1°N, 73.3°E	13.7 (1.4)	11.9 (1.6)	1.8 (1.0)
Buenos Aires, Argentina [34]	34.6°S, 58.5°W	11.82 (0.86)	9.63 (0.92)	2.41 (0.95)
Punta Arenas, Chile [30]	53.1°S, 71°W	9.5	8.8 (7.9)	1.4

the range of 0.5–1.0-km. When compared with results obtained in mid-latitude regions, which are presented in Table 2, Fig. 1(D) indicates that the geometrical thickness of cirrus clouds over SACOL was smaller.

Results presented in Table 2 are compared with measurements derived from lidar systems taken at other latitudes so as to identify similarities and differences in cirrus properties for different latitudinal bands. Table 2 summarizes the observations of cirrus properties and highlights some remarkable differences compared with characteristics noted in other latitudinal bands. From Table 2, it can be seen that the cloud-base and cloud-top height and the cirrus thickness increased with decreasing latitude. The maximum thickness of 2.7 km was observed in Thessaloniki, Greece. However, the mean height values recorded in the present work, both in cloud-base and cloud-top heights, as well as mean thickness values, do not agree with the mean values reported in Table 2. Compared with the findings from studies over other regions, the macrophysical characteristics of cirrus clouds over SACOL tended to be reduced. This comparison may imply differences in the meteorological and geographical conditions between the latitudinal bands. These differences may be caused by the use of different lidar systems and algorithms to retrieve the cirrus clouds properties from lidar measurements.

The frequency distribution of mid-cloud temperatures observed by the TP/WVP-3000 profiling radiometer is presented in Fig. 2. Although temperature observations were confined to the 0−10 km height range, almost 43.6% of observations had a cloud-top height below 10 km. Fig. 2 shows that the temperature of cirrus clouds below 10 km ranged from −53 to −31 °C. Fig. 1(B) and Fig. 2 indicate that the distributions of the cloud-top height and temperature were shifted toward greater height and a lower temperature, with maximums between 9 and 10 km and between −45 and −50 °C, respectively. The distribution of mid-cloud and cloud-base temperatures displayed a maximum between −45 and −50 °C and between −40 and −45 °C, respectively. The mid-latitude cirrus over Oklahoma studied by Wang and Sassen [35] ranged from −40 to −55 °C. Reichardt [16] reported that the frequency distribution of cirrus mid-cloud temperatures ranged between −55 and −60 °C over Geesthacht, Germany. Platt et al. [15] studied the tropical cirrus over Darwin and found that the maximum probability of cirrus mid-cloud temperatures was from

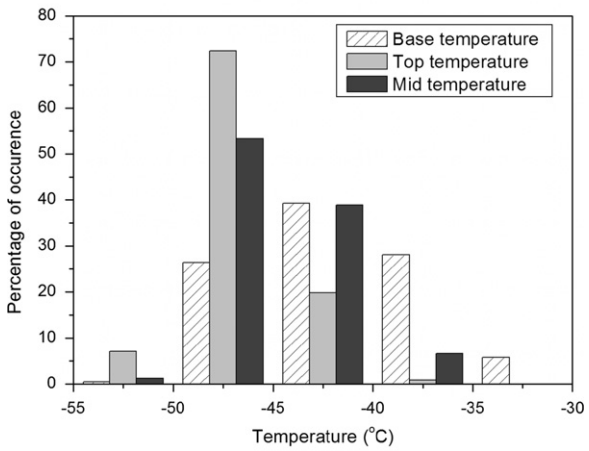

Fig. 2. Frequency distribution of mid-cloud temperature below 10-km height.

−60 to −70 °C. Seifert et al. [33] studied the cirrus over Maldives and found mid-cloud temperatures between −50 and −70 °C. Wider ranges of height and mid-temperature distributions over Chung-Li were reported by Das et al. [32], with the occurrence of cirrus between heights of 8 and 18 km and mid-cloud temperatures between −30 and −80 °C.

4.2. Optical properties

Fig. 3 shows cloud occurrences with different optical depths at intervals of 0.1 km as a probability distribution. The optical depth generally fell between 0.058 and 1.359, with a high probability of 0.1–0.2 optical depth. The probability of occurrence for smaller values of τ was high and decreased with increasing τ. The following estimations of τ can be made from their visual appearance: $\tau \leq 0.03$ for sub-visual, $0.03 \leq \tau \leq 0.3$ for thin, and $0.3 \leq \tau \leq 3.0$ for opaque cirrus clouds [22]. According to Sassen and Cho [22], the optical properties of cirrus and the frequency distributions for cirrus categories are presented in Table 3. Table 3 indicates that the cloud types over SACOL were mainly thin and opaque cirrus. The lidar ratio in thin cirrus, with a value of 32sr, was greater than the lidar ratio in opaque cirrus. Fig. 3 and Table 3 manifest that for 47.2% of samples, the average τ was below 0.3, indicating that half of the cirrus clouds over SACOL were

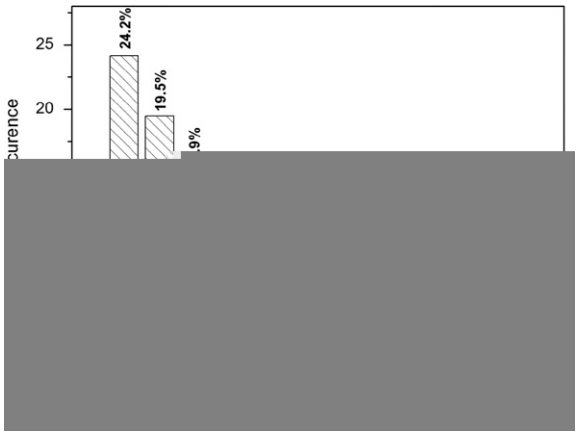

Fig. 3. Frequency distribution of the optical depth of cirrus clouds (0.1-km intervals).

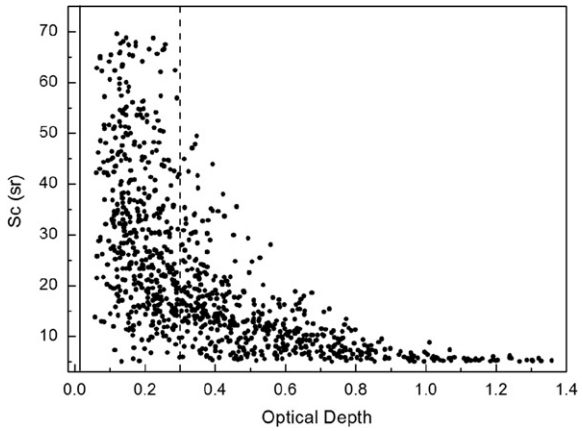

Fig. 4. Scatter plot of the lidar ratio with respect to optical depth at 0.1 intervals. The solid line and dashed line represent optical depth of 0.03 and 0.3, respectively.

Table 3
Statistics of optical properties of cirrus observed over SACOL from April to November 2007.

Cirrus category [22]	S_c (sr)	τ	Corrected S_c (sr)	Corrected τ	Frequency (%)
Sub-visual cirrus ($\tau \le 0.03$)	—	—	—	—	0
Thin cirrus ($0.03 \le \tau \le 0.3$)	32	0.185	35	0.204	47.2
Opaque cirrus ($0.3 \le \tau \le 3.0$)	13	0.581	17	0.843	52.8

optically thin. Giannakaki et al. [19] have found that 60% of the cirrus clouds are sub-visual of optically thin cirrus clouds. Reichardt [16] found that cirrus clouds optical depths are below 0.3 for 70% of the cases studied, while Sassen and Campbell [17] show that cirrus clouds have optical depth lower than 0.3 for 50% of the cases included into their mid-latitude cirrus. The frequency of thin cirrus at SACOL was close to the probability of optically thin cirrus reported by Sassen and Cambell [17]. The errors caused by the proportion of different cloud types observed in different latitudinal bands and sensitivity differences between the different instruments are of low significance.

The data in Table 3 demonstrate that different cirrus categories had different lidar ratios. Similar properties of the lidar ratio are also presented in Fig. 4, which shows a scatter plot depicting the variation in cirrus optical depth with corresponding variations in lidar ratio. To distinguish among the different cirrus categories, a solid and a dashed line are used to differentiate three cirrus categories at the optical depth values of 0.03 and 0.3. The lidar ratio varied from 5 to 70 sr. The lidar ratio of thin cirrus was widely spread through the 5–70 sr range, with a peak appearance below 30 sr. Note that the lidar ratio of opaque cirrus was spread in the 5–50 sr range, with a mean lidar ratio in opaque cirrus of 13 sr. The highest lidar ratio of 32 sr, as shown in Table 3, was found in thin cirrus. It is apparent from Fig. 4 that the peak lidar ratio occurred at an optical depth between 0.058 and 0.3. As the optical depth increased above 0.3 (i.e. opaque cirrus), the lidar ratio decreased exponentially. Sassen and Comstock [36], using LIRAD, calculated the mean lidar ratio to be 25 ± 16 sr for mid-latitude (40.8°N, 111.8°E) cirrus in the USA. Giannakaki et al. [19] derived a lidar ratio of 28 ± 17 sr for mid-latitude (40.6°N, 22.9°E) cirrus in Greece. The mean lidar ratio in cirrus clouds over SACOL was 22 ± 16 sr, which was lower than that in these previous studies because of the lower altitude and frequent occurrence of both thin and opaque cirrus at SACOL. The lidar ratio at SACOL was close to the mean value of 24 sr reported by Min et al. [20].

4.3. Dependencies of cirrus clouds properties

To further investigate the relationship between macrophysical and optical characteristics of cirrus clouds over SACOL, the relationship between cirrus cloud optical and geometrical depth is presented in Fig. 5. Standard errors are shown as vertical bars. Both measured (solid symbol) and values corrected for multiple scattering (hollow symbol) of optical depth are shown. Fig. 5 gives an indication that optical depth increased with increasing geometrical depth. In both cases, the correlation was quite good. The effect of the multiple-scattering correction on the optical depth was so small for thin clouds ($0.03 \le \tau \le 0.3$) that can be ignored; however, the effect of multiple scattering on opaque cirrus ($0.3 \le \tau \le 3.0$) strengthened rapidly with increasing geometrical depth. For comparison, the relationship found during the ICE'89 campaign [37] is also plotted in the same figure (dashed line). The correlation determined by the ICE'89 campaign was lower than the relationship between measured optical depth and geometrical depth in our study when optical depth below 0.3. This finding might be attributed to the 52.8% of opaque cirrus that tended to have greater optical depth.

Fig. 6(A) shows the dependence of the cirrus cloud lidar ratio on mid-cloud height. The lidar ratio plot indicates that the cloud mean lidar ratio fell between 10 and 50 sr, with a turning point at 11–12 km. The cirrus mean lidar ratio at 10–13 km was higher than the mean value in the 5–10-km range. The dependence of optical depth on mid-cloud height is shown in Fig. 6(B). There is an indication that optical depth increased with increasing cloud height in the 5–10-km range. However, when the cloud height increased to 10–13-km range, the optical depth decreased, with a mean value of less than 0.3. Cirrus clouds encountered in the range of 8–10-km height were generally opaque. We should stress that the effect of multiple scattering on the opaque cirrus clouds was of significance. Moreover, the mean value of η was 0.8 ± 0.1 and the lower limit of η was 0.5.

The relationship between mid-cloud height and $1/S_c$ is presented in Fig. 7(A). With the increase of mid-cloud height in the range of 5–9-km, the value of $1/S_c$ decreased linearly. A change occurred in the 9–10-km range. Platt et al. [15] found a change occurring between 8 and 9-km height. Clouds with high temperature are corresponding to high value of $1/S_c$ (Seen in Fig. 7(B)).

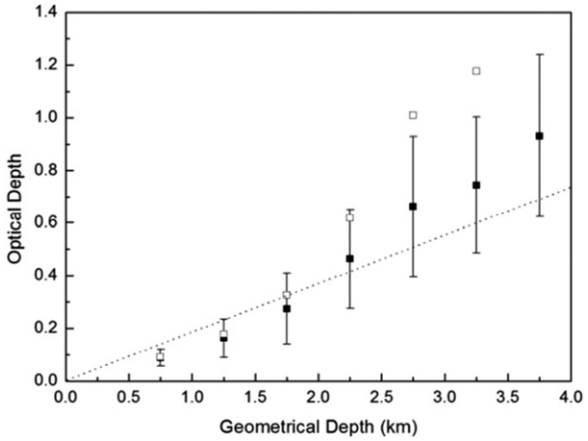

Fig. 5. The relationship between measured (solid symbol) and multiple scattering-corrected (hollow symbol) optical and geometrical depth over 0.5-km intervals. Standard errors are shown as vertical bars. The dashed line represents the regression line given by Ansmann et al. [37].

Fig. 1(C) indicates that 86.8% of cirrus clouds were located below a height of 10 km; the dependences of their optical properties on mid-cloud temperature are demonstrated in Fig. 8, which presents mean values of cloud geometrical depth, lidar ratio, optical depth, and extinction coefficient versus mid-cloud temperature. Fig. 1 indicates that the higher cirrus clouds are also thinner. Consequently, we inferred that the thickness of cirrus clouds was reduced at lower temperatures. Fig. 8(A) indicates that variation in cirrus geometrical depth decreased with mid-cloud temperatures at SACOL, but the standard deviation was just as large, with a maximum again occurring in the -50 to -45 °C range. This result was in qualitative agreement with other cirrus statistics at Aspendale [15] and Thessaloniki [19]. Fig. 8(B) gives the relationship between the lidar ratio and mid-cloud temperature. Although less variation in the lidar ratio was found with variation in mid-cloud temperature, there was a decreasing trend in the standard deviation of the lidar ratio with increasing mid-cloud temperature.

The dependence of optical depth on mid-cloud temperature is shown in Fig. 8(C), and the dependence of the mean extinction coefficient on mid-cloud temperature is presented in Fig. 8(D). Fig. 8(C) and (D) demonstrates that both optical depth and the extinction coefficient showed a strong negative correlation with the mid-cloud temperature. However, our results are in disagreement with results from other studies that showed increased optical depth and extinction coefficient with increased mid-cloud temperature [19,22,36,38]. These discrepancies are likely a consequence of the range observed by the TP/WVP-3000 profiling radiometer, which was confined to 10 km.

5. Summary and conclusions

This paper presents macrophysical and optical characteristics of mid-latitude cirrus clouds using micro-pulse

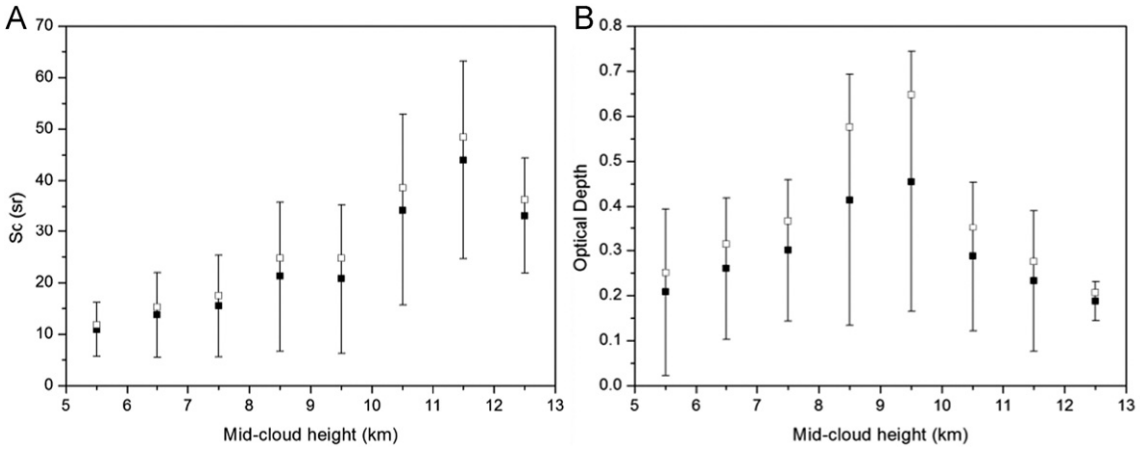

Fig. 6. Dependence of lidar ratio (A) and optical depth (B) on 1-km intervals of mid-cloud height.

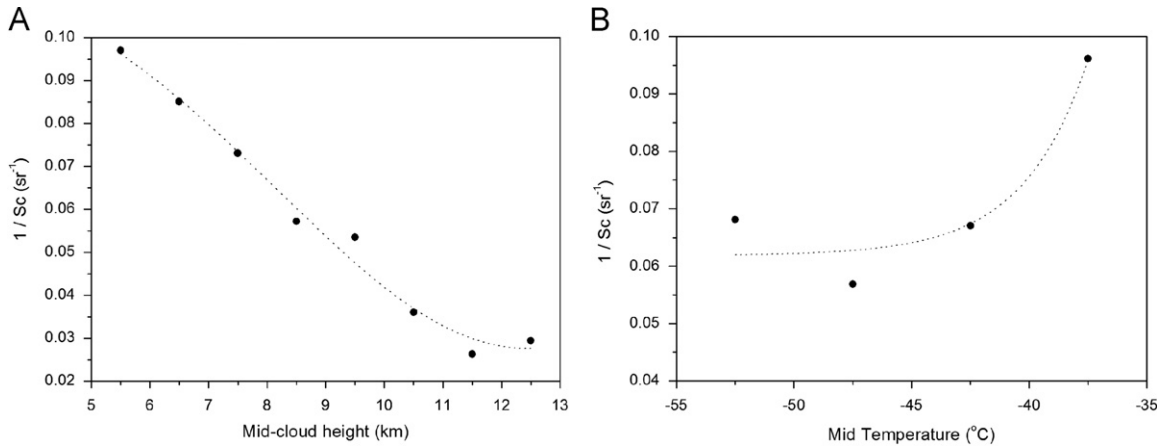

Fig. 7. The relationship between mid-cloud height (A), mid-cloud temperature (B) and $1/S_c$.

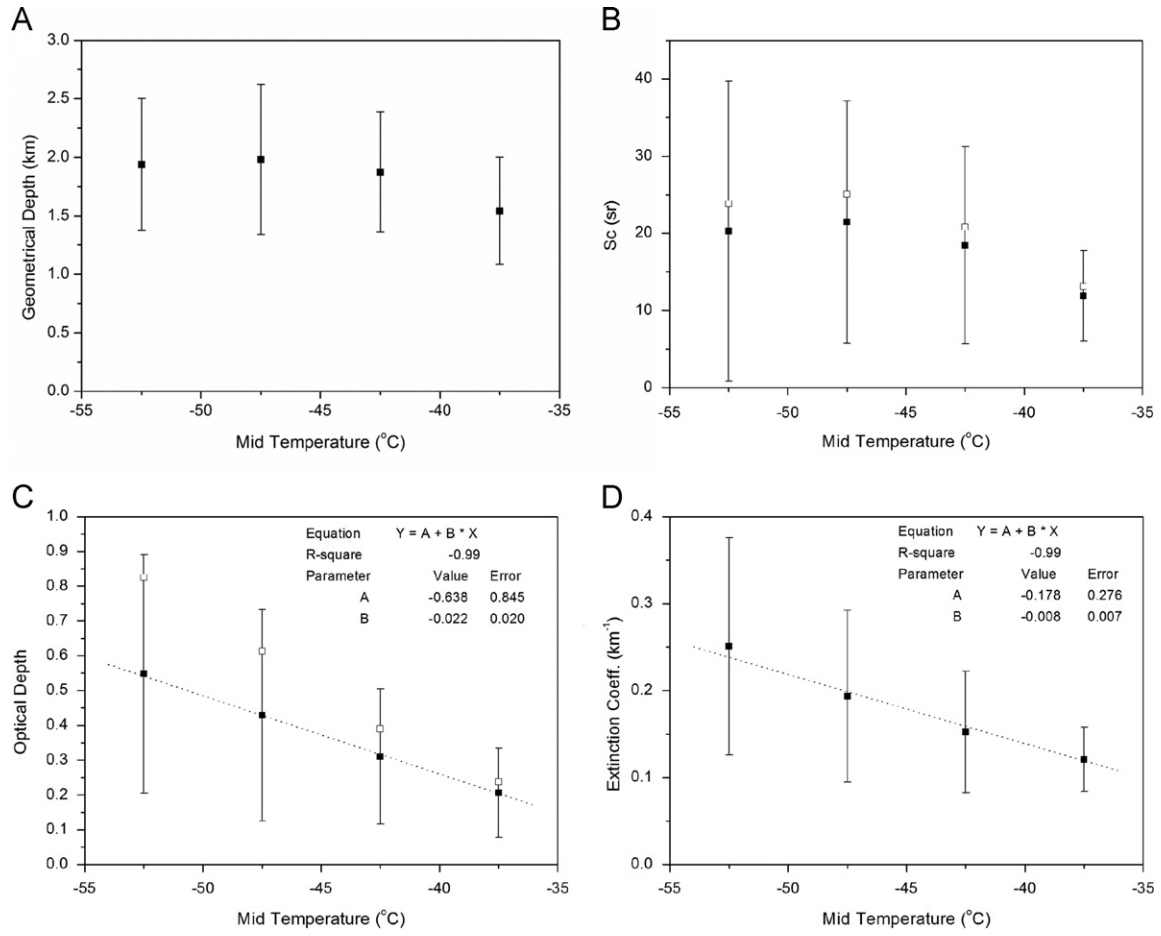

Fig. 8. Mean values of geometrical depth (A), lidar ratio (B), optical depth, (C) and extinction coefficient (D) versus mid-cloud temperature. Values are grouped in intervals of 5 °C. Standard deviations are indicated by vertical bars.

lidar data and profiling radiometer measurements over SACOL in northwest China during the period from April to December 2007. The results are representative of fairly extensive sampling of cirrus clouds at a mid-latitude station. Taking into account these caveats, we summarize the most important features.

Cirrus clouds were generally observed at heights ranging from 5.8 to 12.7 km, with a mean of 9.0 ± 1.0 km.

During the study period, 53.3% of the samples had a temperature between -50 and -45 °C. The cloud geometrical depth ranged from 0.8 to 4.0 km, with a mean thickness of 2.0 ± 0.6 km. Table 2 indicates that the geometrical properties of cirrus clouds measured in our study were reduced compared with results previously reported for mid-latitude cirrus.

Cirrus optical depth at SACOL varied from 0.058 to 1.359, with a mean value of 0.394 ± 0.267, and the most frequent occurrence was between 0.1 and 0.2. The extinction coefficient had a mean value of 0.176 ± 0.084 and a range of 0.048–0.478. The results derived from lidar indicated that the cloud types over SACOL were mostly thin and opaque cirrus. Optical depth increased with increasing geometrical depth up to 10 km. In Fig. 5, the effect of multiple scattering on thin cirrus was of little importance, while the impact on opaque cirrus with small multiple scattering factor was significant. The mean multiple scattering factor was 0.8 ± 0.1, with a lower limit value of 0.5. The dependence of cloud optical depth and the extinction coefficient on mid-cloud temperature was the opposite of findings of previous studies, which is probably attributable to fact that the data from the profiling radiometer were confined to within 10 km. The lidar ratio of cirrus clouds over SACOL varied from 5 to 70 sr, with a mean value of 22 ± 16 sr. The maximum lidar ratio occurred between 0.058 and 0.3 when plotted against optical depth.

Acknowledgments

This research was supported by the National Natural Science Foundation of China (41075104), the National Basic Research Program of China (2012CB955302) and the National Natural Science Foundation of China (41205112). We appreciated all the reviewers for their valuable and critical comments. Thanks were given to the Semi-Arid Climate and Environment Observatory of Lanzhou University (SACOL) for providing lidar data.

References

[1] Liou KN. Influence of cirrus clouds on weather and climate processes: a global perspective. Mon Weather Rev 1986;114:1167–99.
[2] Twomey S. Aerosols, clouds and radiation. Atmos Environ 1991;25:2435–42.
[3] McFarquhar GM, Heymsfield AJ, Spinhirne J, Hart B. Thin and subvisual tropopause tropical cirrus: observations and radiative impacts. J Atmos Sci 2000;57:1841–53.
[4] Heymsfield AJ, McFarquhar GM. Mid-latitude and tropical cirrus. In: Lynch DK, et al., editors. Cirrus, 78. New York: Oxford Univ. Press; 2002. p. 78–101.
[5] Baker MB. Cloud microphysics and climate. Science 1997;276:1072–8.
[6] Ramanathan V, Collins W. Thermodynamic regulation of ocean warming by cirrus clouds deduced from observations of the 1987 El Nino. Nature 1991;351:27–32.
[7] Fu Q, Liou KN. Parameterization of the radiative properties of cirrus clouds. J Atmos Sci 1993;50:2008–25.
[8] Intergovernmental Panel on Climate Change, in Climate Change 2007. The physical science basis. Contribution of working group I to the Fourth Assessment Report of the Intergovernmental Panel on Climate Change. Cambridge, United Kingdom, New York, NY, USA: Cambridge University Press; 2007.
[9] Starr DO. A cirrus cloud experiment: intensive field observations planned for FIRE. Bull Am Meteorol Soc 1987;68:119–24.
[10] Raschke E. Results on cirrus properties from the European Cloud and Radiation Experiment (EUCREX). Preprints, Eighth conference on atmospheric radiation. Nashville, TN: Amer Meteor Soc; 1994. p. 267–78.
[11] Platt CM, Young SA, Carswell AI, Pal SR, McCormick MP, Winker DM, et al. The experimental cloud lidar pilot study (ECLIPS) for cloud-radiation research. Bull Am Meteorol Soc 1994;75(9):1635–54. http://dx.doi.org/10.1175/1520-0477(1994)075<1635:TECLPS>2.0.CO;2.
[12] Nee JB, Len CN, Chen WN, Lin CI. Lidar detection of cirrus cloud in Chung_Li (25°N, 121°E). J Atmos Sci 1998;55:2249–57.
[13] Comstock JM, Ackerman TP, Mace GG. Ground-based lidar and radar remote sensing of tropical cirrus clouds at Nauru Island: cloud statistics and radiative impacts. J Geophys Res 2002;107(D23):4714. http://dx.doi.org/10.1029/2002JD002203.
[14] Pace G, Cacciani M, Sarra AD, Fiocco G, Fuà D. Lidar observations of equatorial cirrus clouds at Mahé Seychelles. J Geophys Res 2003;108(D8):4236. http://dx.doi.org/10.1029/2002JD002 710.
[15] Platt CMR, Scott JC, Dilley AC. Remote sounding of high clouds. Part VI: Optical properties of midlatitude and tropical cirrus. J Atmos Sci 1987;44:729–47.
[16] Reichardt J. Optical and geometrical properties of northern mid-latitude cirrus clouds observed with a UV Raman lidar. Phys Chem Earth Part B 1999;24:255–60.
[17] Sassen K, Cambell JR. A mid-latitude cirrus cloud climatology from the facility for atmospheric remote sensing: part I. Microphysical and synoptic properties. J Atmos Sci 2001;58:481–96.
[18] Xue XL, Qi FD, Fan AY, Liu D, Xie CB, Yue GM, et al. Lidar observations of cirrus clouds over Hefei. Chin J Quantum Electron (in Chinese) 2006;23(4):527–32.
[19] Giannakaki E, Balis DS, Amiridis V, Kazadzis S. Optical and geometrical characteristics of cirrus clouds over a Southern European lidar station. Atmos Chem Phys 2007;7:5519–30.
[20] Min M, Wang PC, Campbell JR, Zong XM, Xia JR. Cirrus cloud macrophysical and optical properties over North China from CALIOP measurements. Adv Atmos Sci 2011;28(3):653–64.
[21] Spinhirne JD. Micropluse lidar. IEEE Trans Geosci Remote Sens 1993;31(1):48–54.
[22] Sassen K, Cho BS. Subvisible-thin cirrus lidar dataset for satellite verification and climatological research. J Appl Meteorol 1992;31:1275–85.
[23] Huang JP, Zhang W, Zuo JQ, Bi JR, Shi JS, Wang X, et al. An overview of the semi-arid climate and environment research observatory over the Loess Plateau. Adv Atmos Sci 2008;25(6):906–21. http://dx.doi.org/10.1007/s00376-008-0906-7.
[24] Hu YX, Rodier S, Xu KM, Sun WB, Huang JP, Lin B, et al. Occurrence, liquid water content, and fraction of supercooled water clouds from combined CALIOP/IIR/ MODIS measurements. J Geophys Res 2010;115:D00H34. http://dx.doi.org/10.1029/2009JD012384.
[25] Doutriaux-Boucher M, Quaas J. Evaluation of cloud thermodynamic phase parameterizations in the LMDZ GCM by using POLDER satellite data. Geophys Res Lett 2004;31:L06126. http://dx.doi.org/10.1029/2003GL019095.
[26] Houze RA. Cloud Dynamics. San Diego: Academic Press; 1993 [573 p.].
[27] Liu RJ, Zhang L, Wang HB, Cao XJ, Huang JP, Bi JR. Cirrus cloud measurement using lidar over semi-arid areas. Chin J Atmos Sci (in Chinese) 2011;35(5):863–70. http://dx.doi.org/10.3878/j.issn.1006-9895.2011.05.06.
[28] Wang X, Boselli A, Avino LD, D'Avino L, Velotta R, Spinelli N, Bruscaglioni P, et al. An algorithm to determine cirrus properties from analysis of multiple-scattering influence on lidar signals. Appl Phys B 2005;80:609–15.
[29] Chen WN, Chiang CW, Nee JB. Lidar ratio and depolarization ratio for cirrus clouds. Appl Opt 2002;41:6470–6.
[30] Immler F, Schrems O. Lidar measurements of cirrus clouds in the northern and southern midlatitudes during INCA (55°N, 53°S): a comparative study. Geophys Res Lett 2002;29(16):1809. http://dx.doi.org/10.1029/2002GL015077.
[31] Goldfarb L, Keckhut P, Chanin M-L, Hauchecorne A. Cirrus climatological results from lidar measurements at OHP (44°N, 6°E). Geophys Res Lett 2001;28:1687–90.
[32] Das SK, Chiang CW, Nee JB. Characteristics of cirrus clouds and its radiative properties based on lidar observation over Chung-Li, Taiwan. Atmos Res 2009;93:723–35.
[33] Seifert P, Ansmann A, Müller D, Wandinger U, Althausen D, Heymsfield AJ, et al. Cirrus optical properties observed with lidar, radiosonde, and satellite over the tropical Indian Ocean during the aerosol-polluted northeast and clean maritime southwest monsoon. J Geophys Res 2007;112:D17205. http://dx.doi.org/10.1029/2006JD008352.

[34] Lakkis SG, Lavorato M, Canziani PO. Monitoring cirrus clouds with lidar in the Southern Hemisphere: a local study over Buenos Aires. 1. Tropopause heights. Atmos Res 2009;92:18–26.
[35] Wang ZE, Sassen K. Cirrus cloud microphysical property retrieval using lidar and radar measurements. Part II: Midlatitude cirrus microphysical and radiative properties. J Atmos Sci 2002;59:2291–302.
[36] Sassen K, Comstock JM. A midlatitude cirrus cloud climatology from the facility for atmospheric remote sensing. Part III: Radiative properties. J Atmos Sci 2001;58:2113–27.
[37] Ansmann A, Bösenberg J, Brogniez G, Elouragini S, Flamant PH, Klapheck K, et al. Lidar network observations of cirrus morphological and scattering properties during the international cirrus experiment 1989: the 18 October 1989 case study and statistical analysis. J Appl Meteorol 1993;32:1608–22.
[38] Sassen K, Wang ZE, Platt CMR, Comstock JM. Parameterization of infrared absorption in midlatitude cirrus clouds. J Atmos Sci 2003;60:428–33.